Journal of Solid State Chemistry 183 (2010) 2534–2543

Contents lists available at ScienceDirect

Journal of Solid State Chemistry

journal homepage: www.elsevier.com/locate/jssc

# The new ternary pnictides $Er_{12}Ni_{30}P_{21}$ and $Er_{13}Ni_{25}As_{19}$: Crystal structures and magnetic properties

Stepan Oryshchyn [a,c], Volodymyr Babizhetskyy [c,*], Olga Zhak [a], Mariya Zelinska [a,b], Jean-Yves Pivan [b], Viola Duppel [c], Arndt Simon [c], Lorenz Kienle [d]

[a] Department of Analytical Chemistry, Ivan Franko National University of Lviv, Kyryla & Mefodija Str. 6, 79005 Lviv, Ukraine
[b] Sciences Chimiques de Rennes UMR CNRS 6226, Université de Rennes 1 - ENSCR, Campus de Beaulieu, Avenue du Général Leclerc, 35042 Rennes Cedex, France
[c] Max-Planck-Institut für Festkörperforschung, Heisenbergstrasse 1, Postfach 800665, D-70569 Stuttgart, Germany
[d] Institute for Materials Science, Synthesis and Real Structure, Christian Albrechts University Kiel, Kaiserstr. 2, D-24143 Kiel, Germany

ARTICLE INFO

*Article history:*
Received 1 July 2010
Received in revised form
12 August 2010
Accepted 15 August 2010
Available online 20 August 2010

*Keywords:*
Rare-earth metal arsenide
Rare-earth metal phosphides
Crystal structure
Electron microscopy
Magnetic behavior

ABSTRACT

The new ternary pnictides $Er_{12}Ni_{30}P_{21}$ and $Er_{13}Ni_{25}As_{19}$ have been synthesized from the elements. They crystallize with hexagonal structures determined from single-crystal X-ray data for $Er_{12}Ni_{30}P_{21}$ (space group $P6_3/m$, $a=1.63900(3)$ nm, $c=0.37573(1)$ nm, $Z=1$, $R_F=0.062$ for 1574 $F$-values and 74 variable parameters), and for $Er_{13}Ni_{25}As_{19}$ ($Tm_{13}Ni_{25}As_{19}$-type structure, space group $P\bar{6}$, $a=1.6208(1)$ nm, $c=0.38847(2)$ nm, $Z=1$, $R_F=0.026$ for 1549 $F$-values and 116 variable parameters). These compounds belong to a large family of hexagonal structures with a metal–metalloid ratio of 2:1. HRTEM investigations were conducted to probe for local ordering of the disordered structure at the nanoscale. The magnetic properties of the phosphide $Er_{12}Ni_{30}P_{21}$ have been studied in the temperature of range $2<T<300$ K and with applied fields up to 5 T. The magnetic susceptibility follows the Curie–Weiss law from 4 to 300 K. The measured value of $\mu_{eff}=9.59\ \mu_B$ corresponds to the theoretical value of $Er^{3+}$.



## 1. Introduction

Recently we have reported some results of systematic investigations in the ternary systems Er–Ni–P and Er–Ni–As at 800 °C [1]. Crystal structures of a number of ternary pnictides have been studied, and solid state phase equilibria have been established. Ternary lanthanoid nickel arsenides $Tb_{12}Ni_{30}As_{21}$ and $Dy_{12}Ni_{30}As_{21}$ were reported by Jeitschko et al. [2] to crystallize with a $(La,Ce)_{12}Rh_{30}P_{21}$-type structure, and the arsenides $Ln_{13}Ni_{25}As_{19}$ ($Ln$=Tm, Y, and Lu) have the crystal structure of the hexagonal $Tm_{13}Ni_{25}As_{19}$ structure type [3]. Babizhetskyy et al. [4] synthesized the ternary rare earth arsenides $R_6Ni_{15}As_{10}$ ($R$=Y, Sm, Gd, Tb, Dy) and investigated their crystal structures. All these compounds as well as many other earlier known ternary phosphides and arsenides described in [5,6] belong to a large structural family with a metal to metalloid ratio equal or close to 2:1.

During our experimental work, two other new phases $Er_{12}Ni_{30}P_{21}$ and $Er_{13}Ni_{25}As_{19}$ have been prepared by high-temperature annealing (1300–1500 °C). The single-crystal X-ray investigation of the $Er_{12}Ni_{30}P_{21}$ and $Er_{13}Ni_{25}As_{19}$ structures proves their relationship with the above mentioned structures of $(La,Ce)_{12}Rh_{30}P_{21}$ and $Tm_{13}Ni_{25}As_{19}$-types, respectively.

Here we present details of the synthesis, crystal structure refinement and measurements of magnetization of the new ternary pnictides $Er_{12}Ni_{30}P_{21}$ and $Er_{13}Ni_{25}As_{19}$. Some preliminary results of this work have been communicated at a conference [7].

## 2. Experimental details

### 2.1. Sample preparation

The compounds were prepared by reaction of the elements. Filings of erbium (nominal purity 99.99%) were mixed with the powders of nickel and red phosphorus or arsenic (all with a stated purity of more than 99.98%) in the definite atomic ratio, pressed into pellets (1 g each) at a pressure of about 5 MPa, put into corundum crucibles and sealed in evacuated silica tubes. All samples were pre-reacted by gradually heating them to 1100 °C (heating rate of 200 °C per day) and keeping the temperature for 3 days, followed by slow cooling to room temperature.

For the synthesis of the phosphide $Er_{12}Ni_{30}P_{21}$ two preparative modes were used. In the first one (I) the pre-reacted sample of the nominal composition $Er_{20}Ni_{42}P_{31}$ was sealed into molybdenum crucible and subsequently heat treated at 1500 °C in a graphite

* Corresponding author. Fax: +49 711 6891091.
*E-mail address:* v.babizhetskyy@fkf.mpg.de (V. Babizhetskyy).

0022-4596/$ - see front matter © 2010 Elsevier Inc. All rights reserved.
doi:10.1016/j.jssc.2010.08.021

furnace for 48 h. In the second mode (II) the powders of the precursors ErP and $Ni_5P_4$ were mixed with the nickel powder in the ratio 12 ErP+2.25 $Ni_5P_4$+18.75 Ni, then pressed into pellet, put into alumina crucible, subsequently sealed into molybdenum crucible, and heat treated at 1500 °C in a graphite furnace for 72 h. According to the XRD data almost all samples contained the mixtures of the phosphides: $Er_{12}Ni_{30}P_{21}$+$Er_{20}Ni_{42}P_{30}$ (synthesis mode I) and $Er_{12}Ni_{30}P_{21}$+$Er_6Ni_{20}P_{13}$ (synthesis mode II). Single crystals of the ternary phosphide $Er_{12}Ni_{30}P_{21}$ were isolated from the crushed samples and tested by Laue method. For the crystal structure determination the single crystals obtained by the mode I were used.

Energy dispersive X-ray spectroscopy analysis (EDXS) of the investigated crystals by a scanning electron microscope JEOL JSM-6400 with an Oxford Link Isis energy-dispersive spectrometer confirmed the presence of only erbium, nickel and phosphorus. The nominal overall composition in atomic percentages measured by EDXS on several crystals was found to be Er:Ni:P=19.2:47.9:32.9 (standard deviation estimated to be about 2 at%), moreover, no contamination by oxygen was detected.

Single crystals of the ternary arsenide $Er_{13}Ni_{25}As_{19}$ were obtained from the pre-reacted and then arc melted sample of composition $Er_{12}Ni_{30}As_{21}$ which was subsequently sealed into a tantalum crucible and heat treated at 1300 °C in a high-frequency furnace (TIG 10/300 Hüttinger). Energy dispersive X-ray spectroscopy analysis of the crystals by scanning electron microscopy (TESCAN 5130MM with Oxford Si-detector) confirmed the presence of only erbium, nickel and arsenic in atomic percentages found to be Er:Ni:As=22.9:44.0:33.1 (standard deviation estimated to be about 1.5 at%). Data of the XRD study of the powdered sample revealed the admixture of the ternary phase $ErNi_4As_2$.

### 2.2. Powder X-ray diffraction

A small part of each sample was pulverized and analyzed by X-ray diffraction (XRD) using a powder diffractometer STOE STADI P using Cu$K\alpha_1$-radiation. Comparison of the obtained diffraction patterns with those corresponding to various structure-types was carried out with the help of the program POWDERCELL [8].

### 2.3. X-ray single crystal structure investigations

*$Er_{12}Ni_{30}P_{21}$*: For the structure determination a prism-shaped single crystal of approx. size $0.1\times0.018\times0.016\,mm^3$ was selected. The intensity data were collected at ambient temperature on a Nonius Kappa CCD diffractometer using monochromatized Mo$K\alpha$ radiation. The unit-cell parameters, orientation matrix as well as the crystal quality were derived from 10 frames recorded at $\chi=0$ using a scan of 1° in $\varphi$. The complete strategy to fill more than a hemisphere was automatically calculated with the use of the program COLLECT [9]. Data reduction and reflection indexing were performed with the program DENZO of the Kappa CCD software package [9]. The scaling and merging of redundant measurements of the different data sets as well as the cell refinement was performed using DENZO. Semi-empirical absorption corrections were made with the use of the program MULTISCAN [10]. Crystallographic data of the phosphide $Er_{12}Ni_{30}P_{21}$ and details of the crystal structure determination are listed in Table 1.

*$Er_{13}Ni_{25}As_{19}$*: Single-crystal intensity data were collected at room temperature on a STOE IPDS image plate diffractometer with monochromatized Ag$K\alpha$ radiation by oscillation of the crystal around the $\omega$ axis. Information about the data collection and evaluations are summarized in Table 1.

**Table 1**
Crystal structure data and structure refinement of $Er_{12}Ni_{30}P_{21}$ and $Er_{13}Ni_{25}As_{19}$.

| | | |
|---|---|---|
| Empirical formula | $Er_{12}Ni_{30}P_{21}$ | $Er_{13}Ni_{25}As_{19}$ |
| Space group | $P6_3/m$ | $P\bar{6}$ (no. 174) |
| *Lattice parameters* | | |
| $a$ (nm) | 1.63900(3) | 1.6208(1) |
| $c$ (nm) | 0.37573(1) | 0.38847(2) |
| $V$ (nm$^3$) | 0.87411(6) | 0.88379(9) |
| Formula units per cell, $Z$ | 1 | 1 |
| Calculated density (g cm$^{-3}$) | 8.3640(5) | 9.493(2) |
| Linear absorption coefficient (mm$^{-1}$) | 46.010 | 33.123 |
| Diffractometer | Nonius Kappa CCD | STOE IPDS I |
| Radiation and wavelength, nm | Mo$K\alpha$ ($\lambda=0.071073$) | Ag$K\alpha$ ($\lambda=0.056086$) |
| $2\theta_{max}$ (deg); $(\sin\theta/\lambda)_{max}$ | 84.23; 0.944 | 56.18; 0.839 |
| Mode of refinement | $F$ ($hkl$), $F(hkl)>4\sigma F(hkl)$ | $F$ ($hkl$), $F(hkl)>4\sigma F(hkl)$ |
| Extinction formalism | Sheldrick-2 0.00188(3) | Sheldrick-2 0.00009(3) |
| Collected reflections | 25,259 | 18,746 |
| Independent reflections | 2002 | 2941 |
| Reflections used in refinement | 1574 | 1549 |
| Refined parameters | 74 | 116 |
| $R_F$; w$R_F$ | 0.062; 0.064 | 0.026; 0.028 |
| Goodness of fit | 1.000 | 1.010 |
| Largest diff.peak and hole (e/Å$^{-3}$) | 6.37[a], −4.73 | 2.48, −1.52 |

[a] Position close to that of the Er1 atoms.

Structure models of the new compounds were determined by Direct Methods using SIR-97 [11]. Refinements and Fourier syntheses were made with the help of the CSD software [12]. The atomic positions were standardized with the help of STRUCTURE TIDY [13].

### 2.4. Electron microscopy studies

Samples were dispersed on perforated carbon foil supported by a copper grid and fixed to a side-entry, double tilt holder with tilting angles of ±25° (Gatan). High resolution transmission electron microscopy (HRTEM), precession electron diffraction (PED) and selected area electron diffraction (SAED) were performed in a Philips CM30ST (300 kV, $LaB_6$ cathode). Diffraction was limited to a circular crystal area of 250 nm. By precession of the electron beam ("Spinning star", NanoMEGAS) multiple scattering was minimized. The EMS packages [14] were used for the simulation of HRTEM micrographs and electron diffraction patterns in kinematic approximation, respectively.

### 2.5. Magnetic measurements

Magnetic measurements were carried out using a MPMS-5 Quantum Design SQUID magnetometer. The magnetization was measured in the temperature range $2<T<300$ K in increasing and decreasing magnetic fields up to 5 T. Moreover, we have not observed any traces of elemental Ni in the samples during the phase purity analysis using X-ray powder diffraction data and the electron microscopy studies.

## 3. Results and discussion

### 3.1. Crystal structure of $Er_{12}Ni_{30}P_{21}$

The phase $Er_{12}Ni_{30}P_{21}$ is the high-temperature phase, as it was mentioned earlier [1]. From the intensity data set, the Laue

**Table 2**
Positional and anisotropic displacement parameters ( $\times 10^2$, $nm^2$) for $Er_{12}Ni_{30}P_{21}$.

| Atom | Site | G | x | y | z | $B_{eq}$ | $B_{11}$ | $B_{22}$ | $B_{33}$ | $B_{12}$ |
|---|---|---|---|---|---|---|---|---|---|---|
| Er1 | 6*h* | 1.0 | 0.36047(2) | 0.23534(2) | 1/4 | 0.546(6) | 0.561(7) | 0.533(7) | 0.533(7) | 0.263(6) |
| Er2 | 6*h* | 1.0 | 0.56117(2) | 0.17753(2) | 1/4 | 0.508(5) | 0.529(7) | 0.483(7) | 0.509(6) | 0.251(6) |
| Ni1 | 6*h* | 1.0 | 0.01421(5) | 0.56467(5) | 1/4 | 0.60(2) | 0.55(2) | 0.58(2) | 0.66(2) | 0.27(2) |
| Ni2 | 6*h* | 0.125(3) | 0.0804(4) | 0.0488(4) | 1/4 | 0.63(6) | – | – | – | – |
| Ni3 | 6*h* | 0.353(4) | 0.1215(2) | 0.0698(2) | 1/4 | 1.10(6) | 0.67(7) | 0.69(7) | 2.14(9) | 0.49(6) |
| Ni4 | 6*h* | 0.521(4) | 0.1523(1) | 0.0891(1) | 1/4 | 0.82(4) | 0.98(5) | 0.64(4) | 0.97(5) | 0.50(4) |
| Ni5 | 6*h* | 1.0 | 0.17993(5) | 0.25196(5) | 1/4 | 0.70(2) | 0.67(2) | 0.63(2) | 0.81(2) | 0.34(2) |
| Ni6 | 6*h* | 1.0 | 0.22931(5) | 0.51267(5) | 1/4 | 0.53(2) | 0.43(2) | 0.45(2) | 0.71(2) | 0.22(2) |
| Ni7 | 6*h* | 1.0 | 0.34679(5) | 0.03860(5) | 1/4 | 0.64(2) | 0.56(2) | 0.60(2) | 0.71(2) | 0.25(2) |
| P1 | 6*h* | 1.0 | 0.0249(1) | 0.2122(1) | 1/4 | 0.61(3) | 0.59(4) | 0.68(4) | 0.59(4) | 0.34(4) |
| P2 | 6*h* | 1.0 | 0.0773(1) | 0.4657(1) | 1/4 | 0.46(3) | 0.53(4) | 0.36(4) | 0.51(4) | 0.24(3) |
| P3 | 6*h* | 1.0 | 0.2800(1) | 0.4114(1) | 1/4 | 0.47(3) | 0.53(4) | 0.37(4) | 0.46(4) | 0.20(3) |
| P4 | 2*c* | 1.0 | 1/3 | 2/3 | 1/4 | 0.42(4) | 0.35(4) | $B_{11}$ | 0.55(7) | $1/2B_{11}$ |
| P5 | 2*a* | 0.26(1) | 0 | 0 | 1/4 | 0.67(9) | – | – | – | – |

Atomic coordinates were standardized using STRUCTURE TIDY [13].

$B_{13} = B_{23} = 0$
$B_{eq} = 1/3(B_{11}a^{*2}a^{*2} + \cdots + 2B_{23}b^*c^*bc\cos\alpha)$,
$T = \exp[-1/4(B_{11}a^{*2}h^2 + \cdots + 2B_{23}b^*c^*kl)$

symmetry 6/*m* was determined, and in accordance with systematic extinctions 0 0 *l* (*l*=2*n*) the centrosymmetric space group $P6_3/m$ was subsequently confirmed. The atomic positions were close to those found earlier for the ternary phosphide $(La,Ce)_{12}Rh_{30}P_{21}$ [15]. After refining the fractional coordinates for all atoms by full-matrix least-squares on *F*, the occupancy factors for the Ni3, Ni4, and P5 positions converged to a partial occupancy of the sites 6*h* located around the $6_3$ axis (52% for Ni4 and 48% for Ni3), and for the 2*a* position in the origin (26% for P5). The abnormally large value for the displacement parameter, $B_{eq}$=4.8, of the Ni3 atom and a high electron density each of about 18.2 e $Å^{-3}$ at a distance of ~0.6 Å to Ni3 further indicate a splitting of this partially occupied position. Finally, the occupancy factors for Ni2, Ni3 and Ni4 atoms were refined to the values listed in Table 2. Anisotropic displacement parameters for all positions occupied by more than 30% were included in the last refinement cycles. Final atomic positional and anisotropic displacement parameters are listed in Table 2. The crystal structure determination led to the composition $Er_{12}Ni_{29.99(1)}P_{20.51(1)}$, close to $Er_{12}Ni_{30}P_{21}$ in good agreement with the result of the EDXS analysis of the single crystals.

Interatomic distances in the $Er_{12}Ni_{30}P_{21}$ structure are listed in Table 3. They come very close to the respective sum of the atomic radii for the metals with coordination number 12, $r_{Er}$=0.1757 nm, $r_{Ni}$=0.1246 nm [16], and the covalent radius of P, $r_P$=0.110 nm [16]. The shortest distances (*d*=0.2197 nm) are observed between atoms Ni6 and P3 corresponding to a contraction of ca. 6.3%.

The projection of the $Er_{12}Ni_{30}P_{21}$ structure onto the *ab* plane and the coordination environment of the atoms are presented in Fig. 1. The large Er atoms are in the centres of hexagonal prisms formed by six nickel and six phosphorus atoms with 6+2 additional Er atoms above all faces (CN=20). Most of the Ni atoms including the deficient sites Ni2, Ni3 and Ni4, have CN=12. Their coordination polyhedra (CP) are distorted orthorhombic prisms with four additional atoms above the rectangular faces. The positions of Ni2, Ni3 and Ni4 are quite close to each other, and hence only mutually one of these positions can be occupied. Since the Ni3 and Ni2 positions have occupation numbers of only 35.3(4)% and 12.5(3)% we have, correspondingly, drawn the coordination polyhedron of the Ni4 position (52.1(4)% occupancy). Only Ni6 centres a trigonal prism formed by six Er atoms with three additional atoms of P and thus has CN=9. The coordination polyhedra of the phosphorus atoms P1–P4 are trigonal prisms of metal atoms with three additional metal atoms above the rectangular faces of the prisms (CN=9). P5 is in the partially occupied crystallographic site 2*a* with CN=6, and the octahedral coordination polyhedron is formed by six Ni atoms situated around the sixfold axis (Ni2, Ni3 or Ni4).

The structure of $Er_{12}Ni_{30}P_{21}$ can be easily derived from the $(La,Ce)_{12}Rh_{30}P_{21}$-type [15] by including one more split-position related to Ni6-atoms, and a reduced occupancy in the 2*a* position. Analysis of the literature data also shows the close relationship between the crystal structures of the ternaries $Tb_{12}Ni_{30}As_{21}$ and $Dy_{12}Ni_{30}As_{21}$ [2], $R_6Ni_{15}As_{10}$ (*R*=Y, Sm, Gd, Tb, Dy) [4], $Y_6Ni_{15-x}P_{10+y}$ (*x*=0.08, *y*=0.15) [17] and the structure of the phosphide $Er_{12}Ni_{30}P_{21}$. The main difference between all these structures is the mode of splitting of the Ni atom position around the sixfold axis and the occupancy factor for P (or As) on this axis. It should be mentioned that octahedral coordination as observed for P5 in the $Er_{12}Ni_{30}P_{21}$ structure is unusual for the metalloid atoms in the related structures of the ternary pnictides [5], but the same polyhedra have been observed for phosphorus and arsenic atoms in partially occupied 2*a* or 2*b* sites in the structures of ternary pnictides reported by Jeitschko et al. [2], Babizhetskyy et al. [4] and Stoyko et al. [17]. In all these structures Ni atoms around the sixfold axes form empty octahedra which can be easily occupied by metalloid atoms.

Closely related structures were also reported for $Nd_3Ni_7P_5$ [18] and $Ce_6Ni_{15}P_{10}$ [19], but in these cases partially occupied positions of the P atoms are absent. Moreover, in the $Nd_3Ni_7P_5$ structure one can observe only one Ni-deficient position (67%) whereas in the $Ce_6Ni_{15}P_{10}$ structure two 6*h* positions are occupied to 79% and 21% by Ni atoms, respectively.

All hexagonal structures mentioned above are members of the large structural family with a metal:metalloid ratio close to 2:1 which has been classified in [5,20,21]. Disregarding the differences concerning the disordered distribution of transition metal atoms (Ni or Rh) and the presence of partially occupied metalloid (P or As) sites these compounds can be derived from the $Fe_2P$-type [22,23] with the general formula $R_{n(n-1)}M_{(n+1)(n+2)}X_{n(n+1)+1}$ [15] (*R*=zirconium, rare earth metal or actinoid; *M*=transition metal; *X*=metalloid) where *n*=4 indicates the number of edge-sharing trigonal prisms around the P or As atoms in one row of the triangular structural fragment with the composition $R_6M_{15}X_{10}$ emphasized in Fig. 1. Some details concerning such types of structure have been widely discussed in [2].

**Table 3**
Interatomic distances ($d$, nm) for the $Er_{12}Ni_{30}P_{21}$ structure [a] with esd.'s given in units of the last significant digit in parentheses.

| Atoms | | $d$ | Atoms | | $d$ | Atoms | | $d$ | Atoms | | $d$ |
|---|---|---|---|---|---|---|---|---|---|---|---|
| **Er1** | 2P1 | 0.2853(1) | **Ni1** | 1Er2 | 0.30589(9) | **Ni4** | 1Ni5 | 0.2475(2) | **Ni7** | 2Ni1 | 0.26830(8) |
| | 2Ni6 | 0.28997(7) | | 1Er1 | 0.3086(1) | | 2Ni5 | 0.2595(1) | | 2Er1 | 0.30274(8) |
| | 2P2 | 0.2910(1) | **Ni2** | 4Ni2 | 0.2202(5) | | [2Ni2 | 0.2639(5)] | | 1Er2 | 0.3087(1) |
| | 2P3 | 0.2924(1) | | 2P5 | 0.2202(4) | | [2Ni2 | 0.2680(6)] | | 1Er1 | 0.31185(9) |
| | 2Ni5 | 0.30160(8) | | [2Ni3 | 0.2394(5)] | | [2Ni3 | 0.2721(3)] | **P1** | 1Ni4 | 0.2211(3) |
| | 2Ni7 | 0.30274(7) | | [2Ni3 | 0.2447(4)] | | [2Ni3 | 0.2750(2)] | | 1Ni7 | 0.2280(2) |
| | 1Ni4 | 0.3035(2) | | [1Ni3 | 0.2485(8)] | | 4Ni4 | 0.2872(2) | | 1Ni5 | 0.2285(2) |
| | 1Ni1 | 0.3086(1) | | [1Ni3 | 0.2536(7)] | | [2P5 | 0.2872(1)] | | [1Ni3 | 0.2290(3)] |
| | 1Ni5 | 0.31042(9) | | 1P1 | 0.2578(7) | | [1Ni2 | 0.2902(7)] | | 2Ni5 | 0.2344(1) |
| | 1Ni7 | 0.31185(9) | | [1Ni4 | 0.2639(5)] | | [1Ni2 | 0.2939(8)] | | 2Ni4 | 0.2346(2) |
| | [1Ni3 | 0.3475(3)] | | [2Ni4 | 0.2680(5)] | | Er1 | 0.3035(2) | | [2Ni3 | 0.2566(2)] |
| | 2Er1 | 0.37573(1) | | 1Ni5 | 0.2885(7) | **Ni5** | 1P1 | 0.2285(2) | | [1Ni2 | 0.2578(6)] |
| | 1Er2 | 0.38375(4) | | [1Ni4 | 0.2902(8)] | | 1P3 | 0.2287(2) | | 2Er1 | 0.2853(1) |
| | 1Er2 | 0.38516(4) | | 2P1 | 0.2906(6) | | 2P1 | 0.2344(1) | | [2Ni2 | 0.2906(5) |
| **Er2** | 2P3 | 0.2876(1) | | [1Ni4 | 0.2939(6)] | | 1Ni4 | 0.2475(2) | **P2** | 1Ni6 | 0.2210(2) |
| | 2P2 | 0.2876(1) | | 2Ni2 | 0.2968(8) | | 2Ni4 | 0.2595(1) | | 2Ni1 | 0.22977(9) |
| | 2Ni6 | 0.29238(7) | **Ni3** | 1P1 | 0.2290(3) | | [1Ni3 | 0.2641(3)] | | 1Ni7 | 0.2317(2) |
| | 2Ni6 | 0.29291(7) | | [2Ni2 | 0.2394(4)] | | 2Ni7 | 0.26639(8) | | 1Ni1 | 0.2319(2) |
| | 2P4 | 0.29367(2) | | [2Ni2 | 0.2447(5)] | | [2Ni3 | 0.2832(2)] | | 2Er2 | 0.2876(1) |
| | 2Ni1 | 0.30241(7) | | [1Ni2 | 0.2485(7)] | | [1Ni2 | 0.2885(8)] | | 2Er1 | 0.2910(1) |
| | 1Ni1 | 0.30589(9) | | [1Ni2 | 0.2536(8)] | | 2Er1 | 0.30160(7) | **P3** | 1Ni6 | 0.2197(2) |
| | 1Ni7 | 0.30872(9) | | [4Ni3 | 0.2555(3)] | | 1Er1 | 0.31042(9) | | 1Ni5 | 0.2287(2) |
| | 2Er2 | 0.37573(1) | | 2P5 | 0.2555(2) | **Ni6** | 1P3 | 0.2197(2) | | 1Ni1 | 0.2298(2) |
| | 1Er1 | 0.38375(4) | | 2P1 | 0.2566(2) | | 1P2 | 0.2210(2) | | 2Ni7 | 0.23136(9) |
| | 1Er1 | 0.38516(4) | | 1Ni5 | 0.2641(3) | | 1P4 | 0.22303(8) | | 2Er2 | 0.2876(1) |
| | 2Er2 | 0.39095(4) | | 2Ni4 | 0.2721(3) | | 2Er1 | 0.28997(7) | | 2Er1 | 0.2924(1) |
| **Ni1** | 2P2 | 0.2298(1) | | 2Ni4 | 0.2750(3) | | 2Er2 | 0.29238(7) | **P4** | 3Ni6 | 0.22303(8) |
| | 1P3 | 0.2298(2) | | 2Ni5 | 0.2832(2) | | 2Er2 | 0.29291(7) | | 6Er2 | 0.29367(3) |
| | 1P2 | 0.2319(2) | | Er1 | 0.3475(3) | **Ni7** | 1P1 | 0.2280(2) | **P5** | [3Ni4 | 0.2172(2)] |
| | 2Ni7 | 0.26830(9) | **Ni4** | 1P5 | 0.2172(2) | | 2P3 | 0.2314(1) | | [6Ni2 | 0.2202(4)] |
| | 2Ni1 | 0.26932(9) | | 1P1 | 0.2211(3) | | 1P2 | 0.2317(2) | | 6Ni3 | 0.2555(2) |
| | 2Er2 | 0.30241(7) | | 2P1 | 0.2346(2) | | 2Ni5 | 0.26639(8) | | [6Ni4 | 0.2872(1)] |

[a] Enclosed in square parentheses are distances for atoms which are not shown in the coordination polyhedra of Fig. 1.

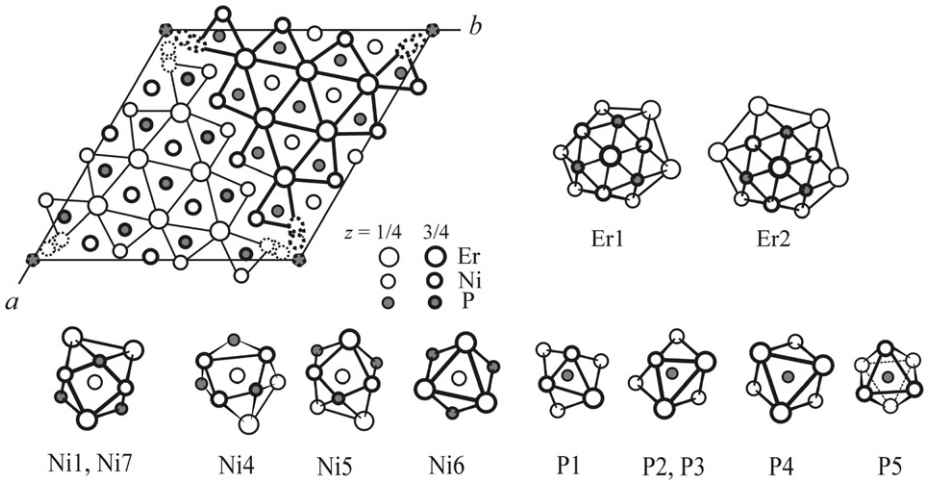


**Fig. 1.** The *ab* projection of the $Er_{12}Ni_{30}P_{21}$ structure and coordination polyhedra of the atoms (positions with partial occupancy are given with dotted lines). Structural fragments $Er_6Ni_{15}P_{10}$ are emphasized.

### 3.2. *Crystal structure of $Er_{13}Ni_{25}As_{19}$*

The crystal structure of $Er_{13}Ni_{25}As_{19}$ was solved by Direct Methods in the space group $P\bar{6}$ (SIR-97 [11]) and refined by full-matrix least-squares on $F$ (CSD software [12]). In the refinement the partial occupancy of Ni2 in the 3*k* position (92.7(9)%) became obvious. All other atom sites are fully occupied by Er, Ni or As atoms. In final least-squares cycles all atoms were refined with anisotropic displacement parameters. Atomic positional and anisotropic displacement parameters are listed in Table 4. The crystal structure determination led to the composition $Er_{13}Ni_{24.78(2)}As_{19}$, as compared to the ideal composition $Er_{13}Ni_{25}As_{19}$. The refined composition of the compound is in good agreement with the data of the EDXS analysis of single crystals.

Analysis of the literature data allows us to attribute the structure of the ternary arsenide $Er_{13}Ni_{25}As_{19}$ to the $Tm_{13}Ni_{25}As_{19}$-type [3] with one difference between these two: in the structure of $Er_{13}Ni_{25}As_{19}$ we observe a fully ordered distribution of atoms in the crystallographic sites with only one partially occupied position, Ni2, whereas in the $Tm_{13}Ni_{25}As_{19}$

**Table 4**
Positional and anisotropic displacement ( $\times 10^2$, $nm^2$) parameters for $Er_{13}Ni_{25}As_{19}$.

| Atom | Site | G | x | y | z | $B_{eq}$ | $B_{11}$ | $B_{22}$ | $B_{33}$ | $B_{12}$ |
|---|---|---|---|---|---|---|---|---|---|---|
| Er1 | 3*k* | 1.0 | 0.03649(5) | 0.29816(5) | 1/2 | 0.46(2) | 0.47(2) | 0.53(2) | 0.37(2) | 0.26(2) |
| Er2 | 3*k* | 1.0 | 0.15278(5) | 0.13249(5) | 1/2 | 0.44(2) | 0.52(2) | 0.47(2) | 0.35(2) | 0.28(2) |
| Er3 | 3*j* | 1.0 | 0.38296(5) | 0.46422(5) | 0 | 0.50(2) | 0.46(2) | 0.56(2) | 0.48(3) | 0.26(2) |
| Er4 | 3*j* | 1.0 | 0.53015(5) | 0.34066(5) | 0 | 0.47(2) | 0.58(2) | 0.50(2) | 0.36(3) | 0.30(2) |
| Er5 | 1*c* | 1.0 | 1/3 | 2/3 | 0 | 0.46(2) | 0.45(2) | 0.45(2) | 0.33(4) | 0.23(2) |
| Ni1 | 3*k* | 1.0 | 0.1548(2) | 0.5319(2) | 1/2 | 0.68(6) | 0.68(7) | 0.78(7) | 0.72(9) | 0.46(6) |
| Ni2 | 3*k* | 0.927(9) | 0.2485(2) | 0.3489(2) | 1/2 | 0.67(7) | 1.11(8) | 0.65(7) | 0.46(9) | 0.59(7) |
| Ni3 | 3*k* | 1.0 | 0.3735(2) | 0.1906(2) | 1/2 | 0.61(6) | 0.53(6) | 0.69(7) | 0.65(8) | 0.32(6) |
| Ni4 | 3*k* | 1.0 | 0.4907(2) | 0.0345(2) | 1/2 | 0.50(5) | 0.44(6) | 0.48(6) | 0.61(8) | 0.24(5) |
| Ni5 | 3*j* | 1.0 | 0.0169(2) | 0.1489(2) | 0 | 0.45(5) | 0.21(6) | 0.41(6) | 0.75(8) | 0.18(5) |
| Ni6 | 3*j* | 1.0 | 0.1950(2) | 0.4403(2) | 0 | 0.58(5) | 0.41(6) | 0.51(6) | 0.58(8) | 0.05(5) |
| Ni7 | 3*j* | 1.0 | 0.3096(2) | 0.2674(2) | 0 | 0.66(6) | 0.69(6) | 0.52(6) | 0.81(9) | 0.33(5) |
| Ni8 | 3*j* | 1.0 | 0.4297(2) | 0.1120(2) | 0 | 0.53(5) | 0.63(6) | 0.63(6) | 0.37(8) | 0.33(5) |
| Ni9 | 1*c* | 1.0 | 2/3 | 1/3 | 1/2 | 0.45(6) | 0.35(6) | 0.35(6) | 0.54(13) | 0.17(6) |
| As1 | 3*k* | 1.0 | 0.2920(1) | 0.5151(1) | 1/2 | 0.45(4) | 0.54(5) | 0.53(5) | 0.41(6) | 0.37(4) |
| As2 | 3*k* | 1.0 | 0.4021(1) | 0.3496(1) | 1/2 | 0.42(4) | 0.48(5) | 0.55(5) | 0.32(6) | 0.33(4) |
| As3 | 3*k* | 1.0 | 0.5212(1) | 0.1947(1) | 1/2 | 0.35(4) | 0.32(4) | 0.31(4) | 0.43(6) | 0.17(4) |
| As4 | 3*j* | 1.0 | 0.0492(1) | 0.4360(1) | 0 | 0.51(4) | 0.59(5) | 0.45(5) | 0.40(6) | 0.20(4) |
| As5 | 3*j* | 1.0 | 0.1660(1) | 0.2763(1) | 0 | 0.44(4) | 0.48(5) | 0.38(5) | 0.45(6) | 0.21(4) |
| As6 | 3*j* | 1.0 | 0.2810(1) | 0.1115(1) | 0 | 0.41(4) | 0.30(4) | 0.41(5) | 0.49(6) | 0.16(3) |
| As7 | 1*a* | 1.0 | 0 | 0 | 0 | 0.45(5) | 0.31(5) | 0.31(5) | 0.61(10) | 0.16(5) |

Atomic coordinates were standardized using STRUCTURE TIDY [13].

$B_{13} = B_{23} = 0$
$B_{eq} = 1/3(B_{11}a^{*2}a^{*2} + \cdots + 2B_{23}b^*c^*bc\cos\alpha)$,
$T = \exp[-1/4(B_{11}a^{*2}h^2 + \cdots + 2B_{23}b^*c^*kl)$

structure the position 3*k* is partially occupied by Ni (93.1%) and the Tm3 position has a mixed Tm/Ni occupancy of 85.6/14.4%.

Interatomic distances in the $Er_{13}Ni_{25}As_{19}$ structure are listed in Table 5. The interatomic distances are again close to the sum of the atomic radii of the metals for the coordination number 12, and the covalent radius of As, $r_{As}$=0.121 nm [16]. The maximal contractions of the interatomic distances are observed between the atoms Er3 and As4 ($d$=0.2716(1) nm), Er3 and Ni7 ($d$=0.2793(2) nm), Ni5 and As5 ($d$=0.2258(2) nm), and Ni5 and As6 ($d$=0.2263(2) nm). In all cases the maximal contraction of interatomic distances is less than 8.5% relative to the sum of the respective radii.

The crystal structure of $Er_{13}Ni_{25}As_{19}$ as well as the structure of $Tm_{13}Ni_{25}As_{19}$ is another member of the large family of planar two layered structures with a metal:metalloid ratio close to 2:1 [3,5,20,21]. The *ab* projection of the $Er_{13}Ni_{25}As_{19}$ structure and the environments of atoms are presented in Fig. 2. As was stated above, the metalloid atoms in these structures are coordinated by trigonal prisms of metal atoms with three additional metal atom neighbors above the rectangular faces of the prisms. So, most of As atoms have trigonal-prismatic coordination and CN=9, only As5 has CN=10 with four additional metal atoms outside the trigonal prism. The same coordination polyhedron was described for the As5 atom in the $Tm_{13}Ni_{25}As_{19}$ structure [3].

Most of the nickel atoms are surrounded by distorted orthorhombic prisms with four additional atoms above their rectangular faces, CN=12. Atoms Ni5 and Ni9 are in the centres of trigonal prisms of Er atoms with three additional As atoms above the rectangular faces of the prisms, CN=9. The large atoms of Er have CN=18 (Er2), and CN=20 (Er1, Er4, and Er5), and their coordination polyhedra are hexagonal prisms with 6 or 8 additional metal atoms above the faces. Only Er3 lies in the centre of a pentagonal prism plus 8 additional atoms, CN=18.

The crystal structure of $Er_{13}Ni_{25}As_{19}$ emphasizing the trigonal prisms of metal atoms in the environment of the As atoms is shown in Fig. 2. The trigonal prisms around As are joined by their edges forming two types of structural fragments with composition $[Er_6Ni_{15}As_{10}]$ and $[Er_9Ni_{10}As_9]$. In the structure the fragments $[Er_6Ni_{15}As_{10}]$ are situated in the channels formed by three blocks of another fragments $[Er_9Ni_{10}As_9]$ which are fused through the atoms of erbium into two dimensional layers. The fragments $[Er_6Ni_{15}As_{10}]$ and $[Er_9Ni_{10}As_9]$ are moved relatively each other by 1/2 *c*.

The fragments $[Er_6Ni_{15}As_{10}]$ ($R_6M_{15}X_{10}$) of the $Er_{13}Ni_{25}As_{19}$ structure are members of a homologous series of the hexagonal two layered structures, and composition of the fragments can be described by the general formula $R_{n(n-1)/2}M_{(n+1)(n+2)/2}X_{n(n+1)/2}$ with $n$=4 [5]. The same structural fragment was also observed in the structure of $Er_{12}Ni_{30}P_{21}$ and other above mentioned compounds. Another fragment of the structure $Er_{13}Ni_{25}As_{19}$ with composition $[Er_9Ni_{10}As_9]$ is composed by a connection of the fragments $[Er_4Ni_3As_3]$ and $[Er_6Ni_7As_6]$. They are derived of $[ErNi_6As_3]$ and $[Er_3Ni_{10}As_6]$ with $n$=2 and 3 in the general formula, respectively. In each fragment described by the general formula three Ni are substituted by three Er, as shown in Fig. 3. Together, they are fused to $[Er_9Ni_{10}As_9]$. Each fragment $[Er_9Ni_{10}As_9]$ has four common atoms of Er with identical neighboring fragments in layers with the composition $[Er_7Ni_{10}As_9]$. Consequently, adding two fragments $[Er_6Ni_{15}As_{10}]$ and $[Er_7Ni_{10}As_9]$ results in the composition of the compound $Er_{13}Ni_{25}As_{19}$.

### 3.3. Characterisation by electron microscopy

Our investigation was performed on the phosphides $Er_{12}Ni_{30}P_{21}$ containing a small amount of $Er_6Ni_{20}P_{13}$ hardly detectable by X-ray powder diffraction, and $Er_{20}Ni_{42}P_{31}$. Starting point of the investigation by electron microscopy was the crystallographic disorder of the Ni atoms around [00*z*] in both $Er_{12}Ni_{30}P_{21}$ and $Er_{13}Ni_{25}As_{19}$. Nanoprobe electron diffraction inside distinct selected areas gave no indication for ordering of the Ni atoms at the nanoscale, in particular neither superstructure reflections nor diffuse scattering were observed. The close similarity of the intensity distributions in the diagrams $Er_{12}Ni_{30}P_{21}$ and $Er_{20}Ni_{42}P_{31}$ along [0 0 1] is particularly interesting.

**Table 5**
Interatomic distances ($d$, nm) for the $Er_{13}Ni_{25}As_{19}$ structure with esd.'s given in units of the last significant digit in parentheses.

| Atoms | | $d$ | Atoms | | $d$ | Atoms | | $d$ | Atoms | | $d$ |
|---|---|---|---|---|---|---|---|---|---|---|---|
| **Er1** | 2As4 | 0.28855(9) | **Er4** | 1Ni8 | 0.3279(2) | **Ni5** | 1As5 | 0.2258(2) | **As2** | 1Ni3 | 0.2377(2) |
| | 2As6 | 0.29795(8) | | 1Er3 | 0.38058(7) | | 1As6 | 0.2263(2) | | 2Ni7 | 0.2406(1) |
| | 2Ni5 | 0.2991(1) | | 2Er4 | 0.38847(2) | | 1As7 | 0.2292(1) | | 1Ni4 | 0.2458(2) |
| | 2As5 | 0.30063(8) | | 2Er4 | 0.39382(7) | | 2Er2 | 0.2990(1) | | 1Ni2 | 0.2483(2) |
| | 1Ni2 | 0.3107(2) | **Er5** | 6As1 | 0.29339(7) | | 2Er1 | 0.2991(1) | | 2Er3 | 0.28107(8) |
| | 2Ni6 | 0.3124(1) | | 3Ni6 | 0.3205(1) | | 2Er2 | 0.3048(1) | | 2Er4 | 0.29003(9) |
| | 1Ni3 | 0.3190(2) | | 6Ni1 | 0.3254(1) | **Ni6** | 1As4 | 0.2327(2) | **As3** | 1Ni9 | 0.2305(1) |
| | 2Ni8 | 0.3229(1) | | 3Er3 | 0.37486(5) | | 2As1 | 0.2410(1) | | 1Ni4 | 0.2354(2) |
| | 1Ni1 | 0.3281(2) | | 2Er5 | 0.38847(2) | | 1As5 | 0.2455(2) | | 1Ni4 | 0.2389(2) |
| | 1Ni4 | 0.3292(1) | **Ni1** | 1As1 | 0.2371(2) | | 2Ni1 | 0.2716(1) | | 2Ni8 | 0.2404(1) |
| | 2Er1 | 0.38847(2) | | 1As1 | 0.2492(2) | | 2Ni2 | 0.2826(2) | | 2Er4 | 0.2999(8) |
| | 2Er2 | 0.39314(7) | | 2As4 | 0.2542(1) | | 1Er3 | 0.2871(2) | | 2Er4 | 0.3006(8) |
| **Er2** | 2As5 | 0.29580(8) | | 1Ni6 | 0.2677(2) | | 2Er1 | 0.3124(1) | **As4** | 1Ni6 | 0.2327(2) |
| | 2As6 | 0.29839(8) | | 2Ni6 | 0.2716(1) | | 1Er5 | 0.3205(1) | | 1Ni8 | 0.2344(2) |
| | 2Ni5 | 0.2990(1) | | 2Er3 | 0.2957(1) | **Ni7** | 1As6 | 0.2329(2) | | 2Ni4 | 0.2486(1) |
| | 2As7 | 0.30334(4) | | 2Er5 | 0.3254(1) | | 2As2 | 0.2406(1) | | 2Ni1 | 0.542(1) |
| | 1Ni2 | 0.3046(2) | | 1Er1 | 0.3281(2) | | 1As5 | 0.2407(2) | | 1Er3 | 0.2716(1) |
| | 2Ni5 | 0.3048(1) | **Ni2** | 2As5 | 0.2319(1) | | 2Ni3 | 0.2772(2) | | 2Er1 | 0.2886(9) |
| | 2Ni7 | 0.3076(1) | | 1As1 | 0.2418(2) | | 1Er3 | 0.2793(2) | **As5** | 1Ni5 | 0.2258(2) |
| | 1Ni3 | 0.3216(2) | | 1As2 | 0.2483(2) | | 2Ni2 | 0.2797(2) | | 2Ni2 | 0.2319(1) |
| | 2Er2 | 0.38847(2) | | 2Ni7 | 0.2797(2) | | 2Er2 | 0.3076(1) | | 1Ni7 | 0.2407(2) |
| | 1Er1 | 0.39314(7) | | 2Er3 | 0.2818(1) | | 1Er4 | 0.3152(2) | | 1Ni6 | 0.2455(2) |
| | 1Er1 | 0.39778(7) | | 2Ni6 | 0.2826(2) | **Ni8** | 1As4 | 0.2344(2) | | 2Er2 | 0.2958(8) |
| **Er3** | 1As4 | 0.2716(1) | | 1Er2 | 0.3046(2) | | 2As3 | 0.2404(1) | | 2Er1 | 0.3006(8) |
| | 1Ni7 | 0.2793(2) | | 1Er1 | 0.3107(2) | | 1As6 | 0.2409(2) | | 1Er3 | 0.309(1) |
| | 2As1 | 0.28008(8) | **Ni3** | 1As3 | 0.2354(2) | | 2Ni3 | 0.2717(1) | **As6** | 1Ni5 | 0.2263(2) |
| | 2As2 | 0.28107(8) | | 1As2 | 0.2377(2) | | 2Ni4 | 0.2751(1) | | 1Ni7 | 0.2329(2) |
| | 2Ni2 | 0.2818(1) | | 2As6 | 0.2400(1) | | 1Er4 | 0.3218(2) | | 2Ni3 | 0.2400(1) |
| | 1Ni6 | 0.2871(2) | | 2Ni8 | 0.2717(1) | | 2Er1 | 0.3229(1) | | 1Ni8 | 0.2409(2) |
| | 2Ni1 | 0.2957(1) | | 2Ni7 | 0.2772(2) | | 1Er4 | 0.3279(2) | | 2Er1 | 0.29795(8) |
| | 2Ni4 | 0.3033(1) | | 2Er4 | 0.3153(1) | **Ni9** | 3As3 | 0.2305(1) | | 2Er2 | 0.29839(8) |
| | 1As5 | 0.3309(1) | | 1Er1 | 0.3190(2) | | 6Er4 | 0.29904(4) | **As7** | 3Ni5 | 0.2292(1) |
| | 1Er5 | 0.37486(5) | | 1Er2 | 0.3216(2) | **As1** | 1Ni1 | 0.2371(2) | | 6Er2 | 0.3033(4) |
| | 1Er4 | 0.38058(7) | **Ni4** | 1As3 | 0.2389(2) | | 2Ni6 | 0.2410(1) | | | |
| | 2Er3 | 0.38847(2) | | 1As2 | 0.2458(2) | | 1Ni2 | 0.2418(2) | | | |
| **Er4** | 2As2 | 0.29003(9) | | 2As4 | 0.2486(1) | | 1Ni1 | 0.2492(2) | | | |
| | 2Ni9 | 0.29904(4) | | 1Ni1 | 02677(2) | | 2Er3 | 0.28008(8) | | | |
| | 4As3 | 0.29993(8) | | 2Ni8 | 0.2751(1) | | 2Er5 | 0.29339(7) | | | |
| | 1Ni7 | 0.3152(2) | | 2Er3 | 0.3033(1) | | | | | | |
| | 2Ni3 | 0.3153(1) | | 2Er4 | 0.3269(1) | | | | | | |
| | 1Ni8 | 03,218(2) | | 1Er1 | 0.3292(1) | | | | | | |
| | 2Ni4 | 0.3269(1) | | | | | | | | | |

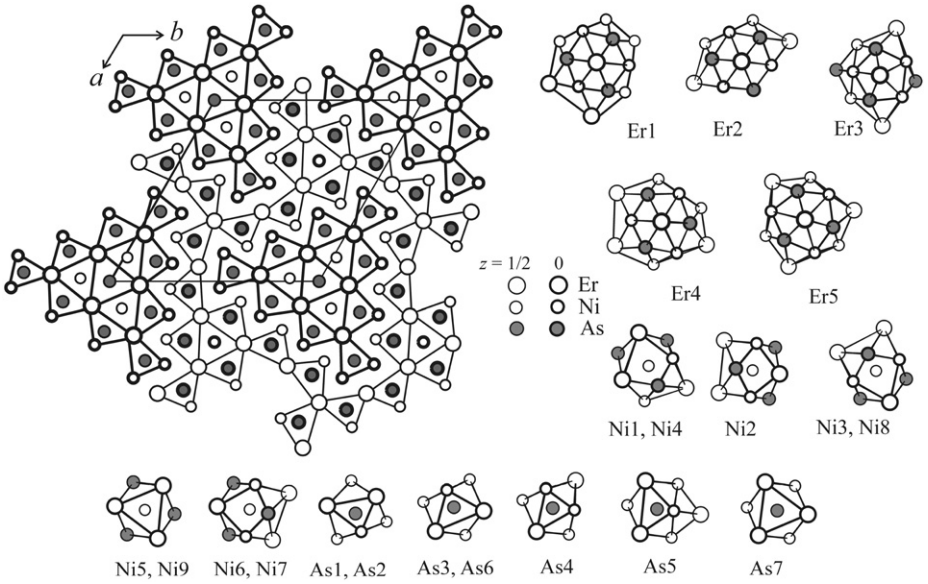


**Fig. 2.** The *ab* projection of the $Er_{13}Ni_{25}As_{19}$ structure and coordination environment of the atoms. Structural fragments $Er_6Ni_{15}As_{10}$ and $Er_9Ni_{10}As_9$ are emphasized.

They correspond to the Fourier transformation of the triangular building blocks with reciprocal scaling of the real object. The observed intensities recorded in the precession mode convincingly agree with calculated data based on the kinematic approximation (cf. Fig. 4), for several zone axes. The slight deviations in terms of too high intensity in the experimental patterns at low resolution are indicative for an incomplete suppression of dynamical effects.

All observed phases belong to the structural series as discussed in Section 3.2 containing triangular building blocks of varying size which are well seen in zone axis [001] (cf. Fig. 5). The triangles contain the heavy Er atoms which strongly contribute to the projected potential and thus dominate the high resolution contrast. The disordered atoms (cf. structure projections in Fig. 5) are located between the triangles. To probe for the experimental significance of a local ordering of the Ni atoms a series of image simulations was performed changing the occupancy factors of the disordered Ni atoms: Ni4, Ni5, Ni6 of $Er_6Ni_{20}P_{13}$; Ni2, Ni3, Ni4 of $Er_{12}Ni_{30}P_{21}$ and Ni7, Ni8 of $Er_{20}Ni_{42}P_{31}$ (cf. Fig. 6). The simulated micrographs only show marginal differences which are expected to fade experimentally by the presence of amorphous surface layers, slight tilts from the precise zone axis orientation and other unavoidable experimental drawbacks. The experimental micrographs presented in Fig. 5 match the inserted simulations based on the average structures (see X-ray analyses). Fourier transforms of

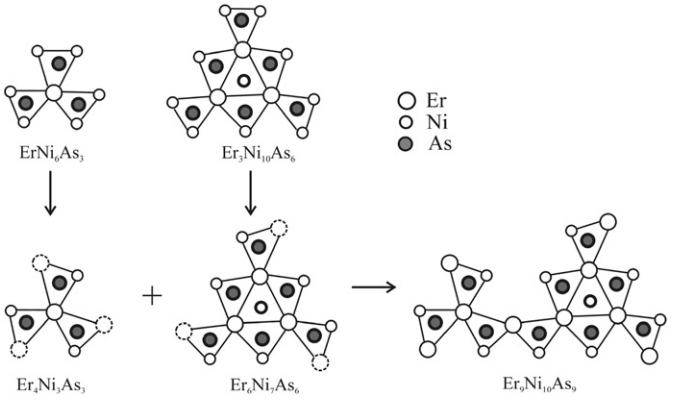


**Fig. 3.** Mode of formation of the structural fragment $[Er_9Ni_{10}As_9]$ present in the crystal structure of the ternary arsenide $Er_{13}Ni_{25}As_{19}$ (positions where the nickel atoms are substituted by erbium atoms are given by dotted lines).

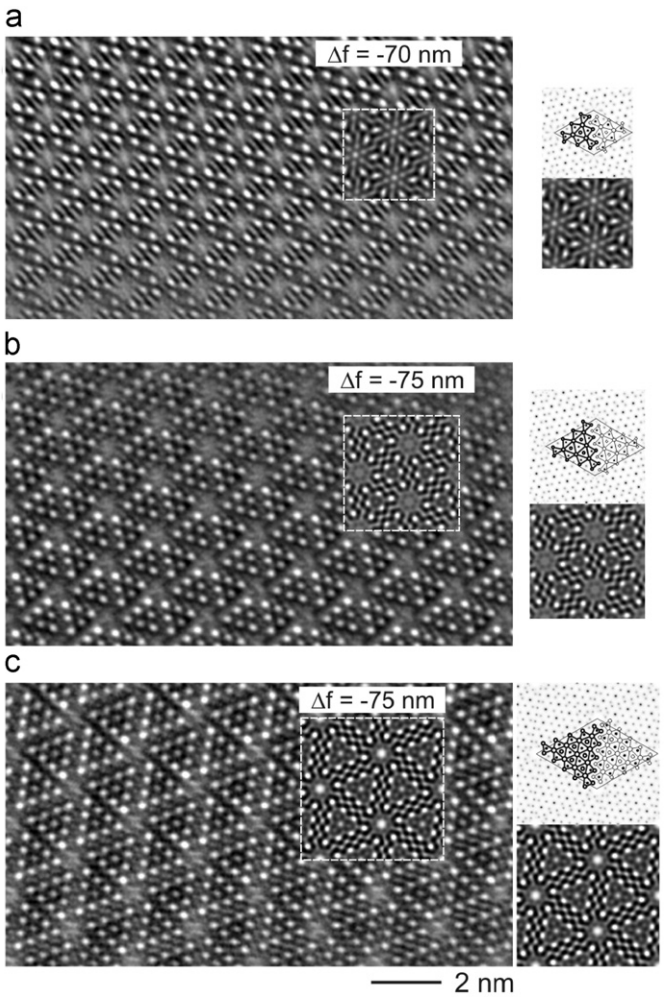


**Fig. 5.** HRTEM of (a) $Er_6Ni_{20}P_{13}$, (b) $Er_{12}Ni_{30}P_{21}$ and (c) $Er_{20}Ni_{42}P_{31}$ with inserted simulations ($t$=2.2 nm (a) and $t$=2.3 nm (b) and (c)). Zone axis orientation [001].

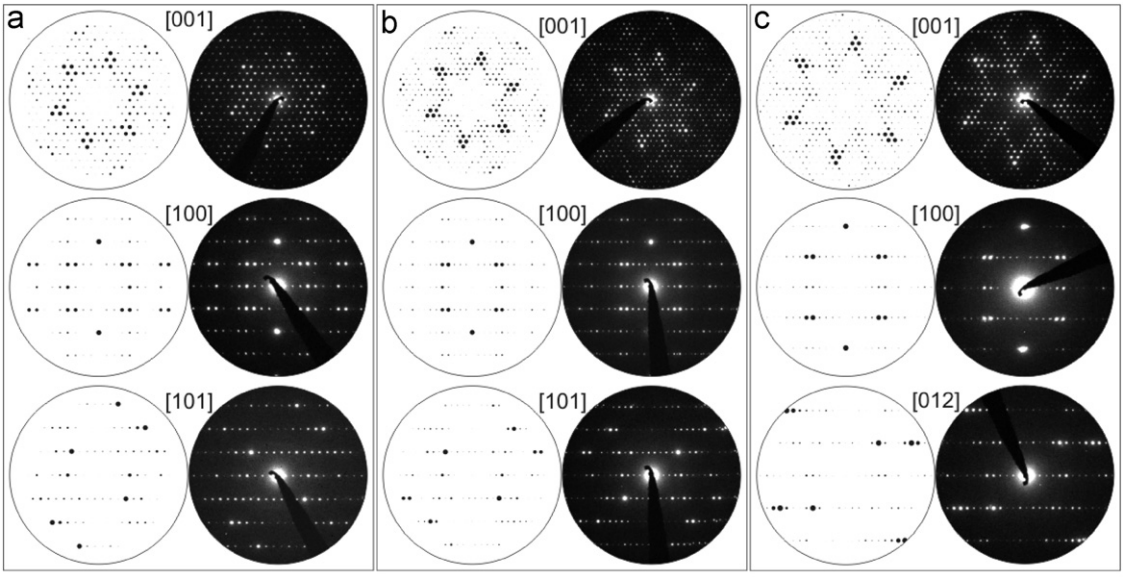


**Fig. 4.** Simulated (left) and experimental (right) PED diagrams for (a) $Er_6Ni_{20}P_{13}$, (b) $Er_{12}Ni_{30}P_{21}$ and (c) $Er_{20}Ni_{42}P_{30}$.

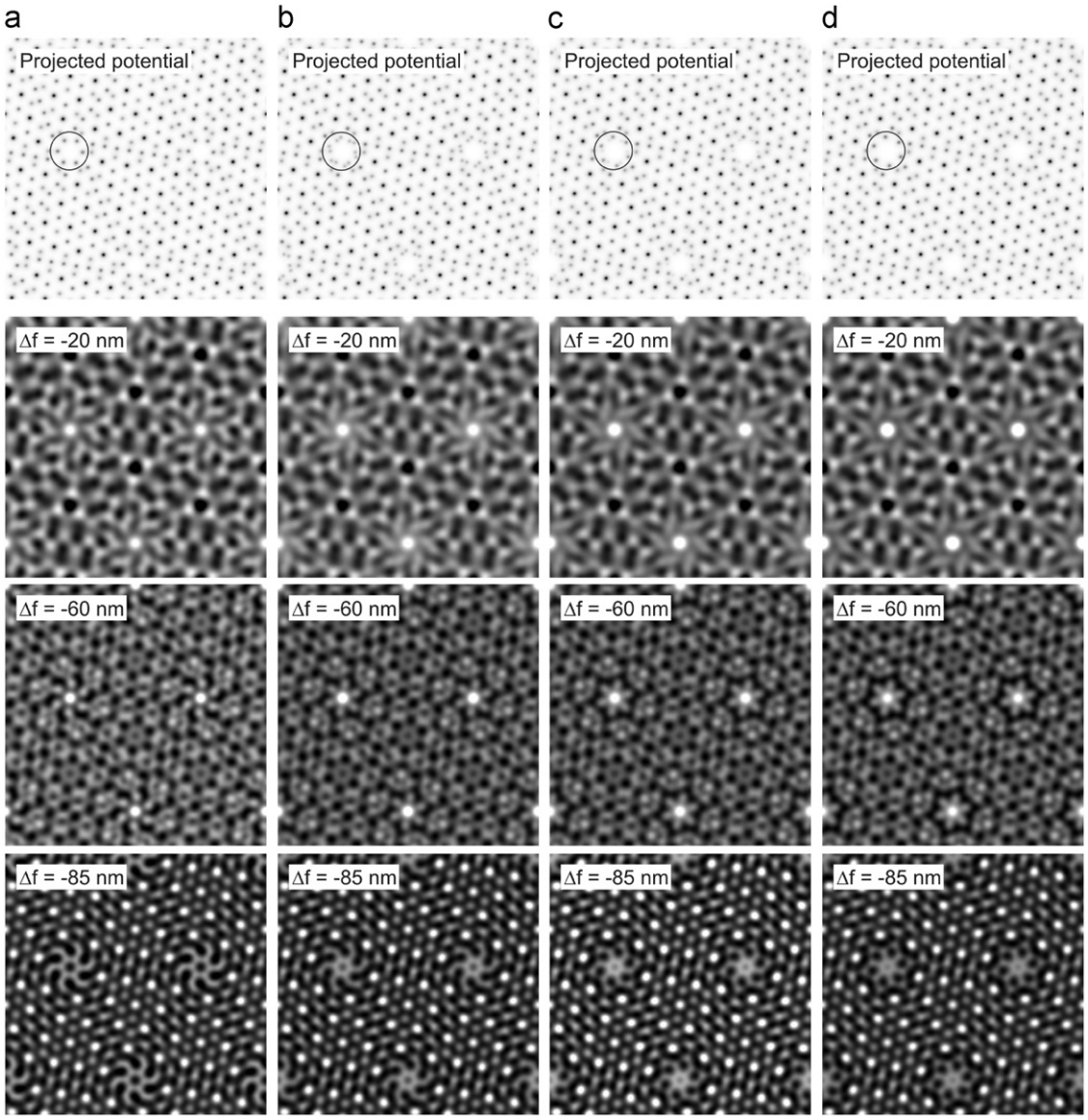


**Fig. 6.** Image simulations series $Er_{20}Ni_{42}P_{31}$ in zone axis [001] with different Ni atom ordering: (a) occupancy: Ni 7: 0%, Ni 8: 100%, (b) Ni 7: 50%, Ni 8: 50%, (c) Ni 7: 77%, Ni 8: 18% and (d) Ni 7: 100%, Ni 8: 0%.

the micrographs do not show any anomalies. However, this finding does not exclude local ordering of the disordered Ni atoms on an atomic scale as indicated by its low experimental significance. As expected from the contributions to the projected potential, the Er atoms are imaged as bright spots in strongly underfocused high-resolution images ($\Delta f < -60$ nm). Depending on the chemical nature of the examined crystal, these spots form triangles with increasing sizes in the series $Er_6Ni_{20}P_{13}$, $Er_{12}Ni_{30}P_{21}$ and $Er_{20}Ni_{42}P_{31}$. Based on the triangular building blocks there could be a distinctly different origin of disorder, somewhat related to the intergrowth of packets with varying sizes as studied in detail for the intersecting vacancy layers of $Ga_2Te_3$ [24]. However, such disordering and other, more significant features of local ordering were not observed. The full defocus series can be seen in Fig. 7.

Thus, the images clearly indicate that the investigated crystals are built from uniform triangular blocks. The disorder around 00*z* observed in the X-ray structure analyses is based on local ordering on the atomic scale, most probably related to mutual substitutions of the smaller kind of atoms, Ni and P, in the region of six adjacent triangular blocks.

### 3.4. Magnetic properties of $Er_{12}Ni_{30}P_{21}$

The magnetic susceptibility of $Er_{12}Ni_{30}P_{21}$ follows the Curie–Weiss law over the entire temperature range between $2 < T < 300$ K (Fig. 8). The effective magnetic moment is in good agreement with the theoretical value, calculated for the trivalent free ion $\mu_{eff}=9.59\ \mu_B/Er^{3+}$.

The *M*–*H* curve was measured at 2 K whereas the *M*–*T* (or $(1/\chi)$–*T*) measurement has been done from 5 to 300 K. The graph depicting $(1/\chi)$–*T* behavior shows a perfect paramagnetic nature of sample down to 5 K. An extrapolation of the straight line however, shows a positive Curie–Weiss content 1.90(10) K suggesting ferromagnetic ordering below 5 K. This is confirmed by *M*–*H* measurements performed at 2 K. We have not observed any traces of elemental Ni in the sample during the phase purity

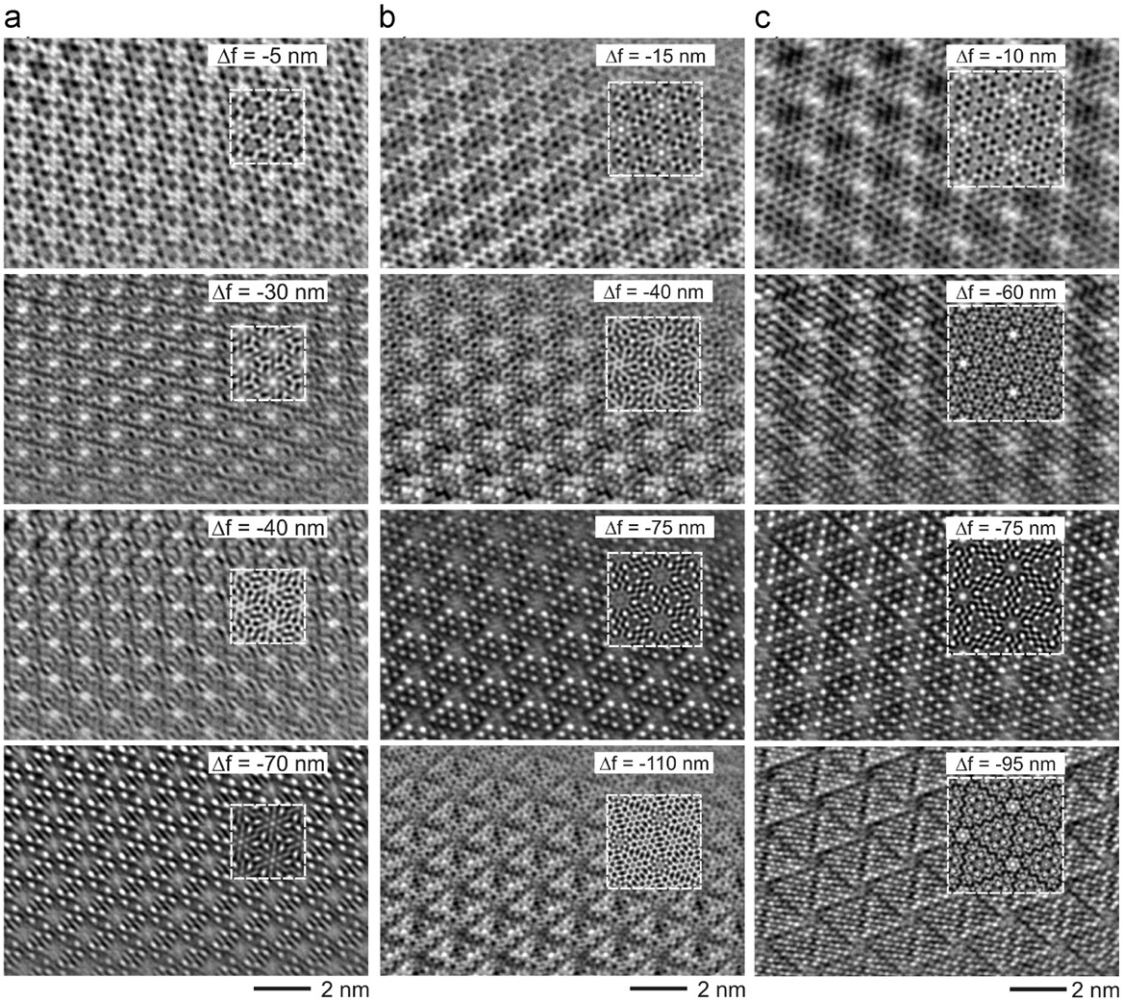


**Fig. 7.** The full HRTEM series of (a) $Er_6Ni_{20}P_{13}$, (b) $Er_{12}Ni_{30}P_{21}$ and (c) $Er_{20}Ni_{42}P_{31}$ with inserted simulations ($t$=2.2 nm (a) and $t$=2.3 nm (b and c)). Zone axis orientation [001].

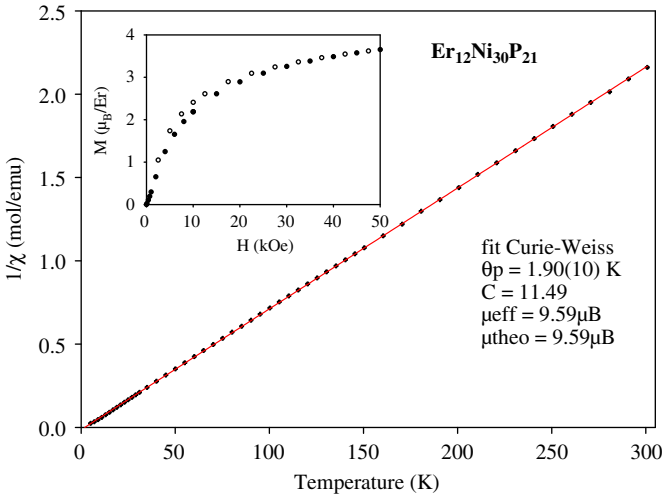


**Fig. 8.** Temperature dependence of the magnetic susceptibility ($1/\chi$) for $Er_{12}Ni_{30}P_{21}$. The solid line represents the fit of the data to the Curie–Weiss law. The inset in the top-left corner presents the field dependence of the magnetization $M=f(H)$ recorded at 2 K with increasing (●) and decreasing (○) field.

analysis. The strongly reduced magnetic moment at 2 K could be due to the crystal field effect preventing the perfect alignment of the Er moments.

## 4. Conclusion

The new ternary pnictides $Er_{12}Ni_{30}P_{21}$ and $Er_{13}Ni_{25}As_{19}$ were synthesized from the elements. They crystallize with hexagonal structures belong to a large family of hexagonal structures with a metal–metalloid ratio close to 2:1. The crystal structure of the phosphide $Er_{12}Ni_{30}P_{21}$ is closely related with the $(La,Ce)_{12}Rh_{30}P_{21}$-type, and the structure of the arsenide $Er_{13}Ni_{25}As_{19}$ is a new representative of $Tm_{13}Ni_{25}As_{19}$-type. The magnetic properties of the phosphide $Er_{12}Ni_{30}P_{21}$ in the range $2<T<300$ K and with applied fields up to 5 T have been studied. The magnetic susceptibility of the compound follows the Curie–Weiss law in a large temperature range.

## Supplemental information

Further details of the crystal structure investigation can be obtained from the Fachinformationszentrum Karlsruhe, 76344 Eggenstein-Leopoldshafen, Germany (fax: (49)7247-808-666; E-mail: crystdata@fiz-karlsruhe.de) on quoting the depository numbers CSD-421919 for $Er_{13}Ni_{25}As_{19}$ and 421920 for $Er_{12}Ni_{30}P_{21}$.

## Acknowledgments

The authors gratefully thank Dr. C. Hoch (Max-Planck-Institut für Festkörperforschung) and T. Roisnel (CDIFX, Université de Rennes 1) for X-ray intensity data collection.

## References


[1] M. Zelinska, O. Zhak, S. Oryshchyn, T. Polianska, J.-Y. Pivan, Z. Naturforsch. 62b (2007) 1143.
[2] W. Jeitschko, L.J. Terbüchte, U.Ch. Rodewald, Z. Anorg. Allg. Chem. 627 (2001) 2673.
[3] W. Jeitschko, L.J. Terbüchte, U.Ch. Rodewald, Z. Anorg. Allg. Chem. 627 (2001) 2095.
[4] V. Babizhetskyy, K. Hiebl, A. Simon, J. Alloys Compd. 413 (2006) 17.
[5] Yu B. Kuz'ma, S.I. Chykhrij, in: K.A. Gschneinder Jr, L. Eyring (Eds.), Handbook of the Physics and Chemistry of Rare Earths, vol. 23, Elsevier Science, Amsterdam1996, pp. 285–434 (Phosphides) (Chapter 156).
[6] P. Villars, in: Pearson's Handbook, Desk Edition, The Materials Information Society, Materials Park, OH, 1997.
[7] H. Noël, S.V. Oryshchyn, J.-Y. Pivan, M. Potel, O. Tougait, O.V. Zhak, M.V. Zelinska, in: Book of Abstract of 15th International Conference on Solid Compounds of Transition Elements, Krakow, 2006, p. 14.
[8] W. Krause, G. Nolze, J. Appl. Crystallogr. 29 (1996) 301.
[9] Nonius, in: Collect, Denzo, Scalepack, Sortav, Kappa CCD Program Package, Nonius BV, Delft, The Netherlands, 1998.
[10] R.H. Blessing, Acta Crystallogr. 51 (1995) 33.
[11] A. Altomare, M.C. Burla, M. Camalli, G.L. Cascarano, C. Giacovazzo, A. Guagliardi, A.G.G. Moliterni, G. Polidori, R.J. Spagna, J. Appl. Crystallogr. 32 (1999) 115.
[12] L.G. Akselrud, Yu.N. Grin, V.K. Pecharsky, P.Yu. Zavalij, CSD97-Universal program package for single crystal and powder data treatment, version no. 7, 1997.
[13] L.M. Gelato, E. Parthé, STRUCTURE TIDY—a computer program to standardize crystal structure data, J. Appl. Crystallogr. 20 (1987) 139.
[14] P. Stadelmann, Ultramicroscopy 21 (1987) 131–146.
[15] J.-Y. Pivan, R. Guérin, J. Less-Common Met. 120 (1986) 247.
[16] J. Emsley, in: Die Elemente, de Gruyter, Berlin, 1994.
[17] S. Stoyko, S. Oryshchyn, V. Babizhetskyy, R. Guérin, J. Alloys Compd. 367 (2004) 156.
[18] S.I. Chykhrij, S.V. Oryshchyn, Yu.B Kuz'ma, T. Glowiak, Sov. Phys. Crystallogr. 34 (1989) 1131 (in Russian).
[19] V.S. Babizhetskyy, S.I. Chykhrij, S.V. Oryshchyn, Yu.B Kuz'ma, Ukr. Khim. Zhurn. 59 (1993) 240 (in Ukrainian).
[20] J.-Y. Pivan, R. Guérin, J. Solid State Chem. 135 (1998) 218.
[21] Yu.M. Prots', W. Jeitschko, Inorg. Chem. 37 (1998) 5431.
[22] S. Rundqvist, F. Jellinek, Acta Chem. Scand. 13 (1959) 425.
[23] B. Carlsson, M. Gölin, S. Rundqvist, J. Solid State Chem. 8 (1973) 57.
[24] V. Duppel, A. Simon, H.J. Deiseroth, Z. Anorg. Allg. Chem. 629 (2003) 1412.